https://chemclassjournal.com/
ChemClass Journal Vol. 9 Issue 2 (2025); 382-395
e-ISSN:3092-8214 p-ISSN:3092-8206
DOI: https://doi.org/10.33003/chemclas-2025-0902/166

Detoxification of Cr (VI), Mn (II) and Pb (II) Ions from Mining Wastewater by Sorption onto Chemically Modified Agricultural Wastes

***Musah, M., [1]Azeh, Y., [1]Mathew, J. T., [1]Badeggi, U. M., [1]Muhammad, A. I., [2]Abu, L. M., [1]Muhammad, H. I., [1]Muhammad, K. T. and [1]Muhammad, H. A.**

**[1]Department of Chemistry, Ibrahim Badamasi Babangida University, Lapai, Nigeria*

[2]Department of Biochemistry, Ibrahim Badamasi Babangida University, Lapai, Nigeria

(*) Corresponding author: mkwagana@gmail.com; mmusah@ibbu.edu.ng
Phone: +234(0)8034064331

Abstract

The removal of Cr (VI), Mn (II) and Pb (II) ions from mining wastewater onto activated carbon prepared from the seed shells of *Vitellaria paradoxa* (VPA) and *Mangifera indica* (MIA) was studied using the batch adsorption method at 20, 40, 60, 80 and 100 minutes and 250 rpm. The influence of contact time was used to determine experimental, qe(exp) and theoretical, qe(cal) values. Four adsorption kinetic models: pseudo first-order, pseudo second-order, Natarajan-Khalaf first order and Bhattacharya-Venkobachar first order were tested. The values of correlation coefficient, R^2 and rate constant, k for the pseudo second order kinetics for the adsorption of Cr (VI) were 0.9847 (VPA) and 0.3632 (VPA) respectively, and were higher than R^2 and k values obtained for pseudo first order (0.9770 and 0.0212), Natarjan and Khalaf first order (0.9713 and 0.0083), and Bhattacharya and Venkobachan kinetics (0.8558 and 0.0205). The sum of square of error calculated to compare the fitness of the adsorption kinetics indicated that the adsorption of Cr (VI) followed the pseudo second order kinetics. Similar trend was observed for R^2 and k values for the adsorption of Mn (II) and Pb (II) form mining wastewater. McKay and Poots intraparticle and Weber and Morris intraparticle diffusion were also tested. Correlation coefficient (R2) values obtained for the diffusion of Cr (VI), Mn (II) and Pb (II) using the McKay - Poots model were 0.9993, 0.9417 and 0.9029 respectively. Values obtained for McKay - Poots intraparticle rate constant, kid (mg.g-1min-1) 0.0037, 0.0239 and 0.0016 for VPA. Lower kid values (0.0037, 0.0237 and 0.0016) were obtained for the adsorption of the metal ions onto VPA. Weber and Morris intraparticle rate constant, k1 (mg/gmin1/2) for the adsorption of Cr (VI), Mn (II) and Pb (II) onto VPA were 0.0174, 0.0552 and 0.0096 respectively. Correlation coefficient (R^2) values were in the order: 0.9866 > 0.9439 > 0.9175 for adsorption onto VPA. Results obtained from this study indicate that the adsorption of Cr (VI), Mn (II) and Pb (II) onto the adsorbent follows the pseudo second order adsorption kinetic and intraparticle diffusion is predominantly the McKay - Poots model. Correlation coefficient of the experimental values indicate good performance of the models. These models can be employed to monitor the removal of heavy metal pollutants from industrial effluent.

Keywords: Detoxification, adsorption, ions, kinetics, diffusion, wastewater, seed shells

Introduction

Heavy metals can enter the environment through natural or anthropogenic processes. These metals can persist in the environment for very long time thereby contributing to problems of pollution of the environment and contamination of water sources. Environmental pollution by heavy metals is very common in locations of mining and areas that were mine sites in the past. Mining involves the extraction or removal of minerals or geological deposits from the earth. The metals and minerals mined have found their applications in various sectors like housing, telecommunication, construction and space exploration. Pollution of water bodies has been a major concern associated with mining activity [1,2]. The large quantities of wastewater produced from mining activities such as mine cooling, aqueous extraction, mine drainage are known to increase the likelihood of discharging of contaminant into the environment and the possibilities for the contamination of surface water and ground by heavy metals [3,4].

In many developing countries including Nigeria, most extraction industries discharge their wastewaters into the environment without any form treatment and there is little or no supervision by authorities responsible for monitoring and enforcing laws on the treatment and discharge of wastewater into the environment [5]. Different chemical and physical processes exist for industrial wastewaters treatment to remove heavy metals. These methods include reverse osmosis, coagulation, electrolytic recovery, evaporation-recovery, electrochemical precipitation, ion exchange, ultrafiltration and biological techniques [6,7]. Sludge formation and precipitation are major militating factors in some of these processes. While ion exchange is considered a good method that can remove heavy metal from solutions, its high operational cost makes it an unappealing method. Considering these factors, the use of activated carbon prepared from low-cost agricultural wastes with high viability as adsorbent to remove noxious heavy metal from wastewater have recently been emphasized [8].

Adsorbent prepared from agricultural wastes mostly of plant origin have been reported to be industrially viable for the adsorption of heavy metal pollutants from solutions [9,10]. Agricultural wastes represent a great number of unused materials which possess features that make them suitable precursors for activated carbon [11]. Activated carbon (AC) is one of the most commonly used adsorbents for wastewater treatment. Activated carbon is a highly porous carbonaceous material with surface area of over 500 m^2/g. It consists of an unequal array of micro crystallite that are interconnected, and each be made up of fused hexagonal ring of carbon that are similar to the structure graphite. AC is mainly an amorphous solid which consist of high pore volume and large internal surface area [12].

Any adsorbent that exhibits good selective ability and high capacity for adsorption is considered very significant in the removal of adsorbate from wastewater. This study seeks to determine the suitability of activated carbons from *Vitellaria paradoxa* and *Mangifera indica* nut shell wastes for the adsorption of Cr (VI), Mn (II) and Pb (II) ions from mining wastewater.

Materials and Methods

Adsorbents used in this study were prepared from *Vitellaria paradoxa* and *Mangifera indica* nut shell wastes using the two step activation method with phosphoric acid as the activating agent, coded as VPA and MIA. Mining wastewater was collected from a local mining site around Chanchaga area in Minna, Nigeria. The wastewater is released into water body after washing of the dug soil to obtain crude gold.

Batch Adsorption of Metal Ions

Adsorbent earlier prepared and characterized was used for the study. Batch adsorption was employed for adsorption of Cr (VI), Mn (II) and Pb (II) from the mining wastewater. Using this method, 0.2 g of adsorbent, *Vitellaria paradoxa* shell activated carbon (VPA) and *Mangifera indica* shell activated carbon (MIA) interacted with 20 cm^3 of the wastewater. The mixture was allowed to shake for 20 minutes at 250 rpm; the adsorbate-adsorbent interaction was repeated for 40, 60, 80 and 100 minutes. The mixtures were filtered using Whatman filter paper (No.42), each filtrate was collected separately into a labelled sample bottle.

Digestion of Wastewater

After interaction with the adsorbent, the wastewater was digested to ensure organic impurities were removed and to also prevent the interference of impurities during analysis of the sample. Wet digestion was employed for digesting the wastewater. In this method, 5cm^3 of concentrated HNO_3 was added into the sample in a 250 cm^3 beaker. The mixture was heated on a hotplate to evaporate, followed by the addition of 5 cm^3 of HNO_3 and was heated under reflux. The process continued until clear solution was obtained. 2 cm^3 of conc. HNO_3 was further added to the precipitates to dissolve. After cooling, the apparatus was rinsed thoroughly and the digest was poured into a volumetric flask (100 cm^3) and the volume made up to mark [13].

Concentration of each heavy metal ion in the wastewater was determined before and after interaction with the adsorbents using Atomic Absorption Spectrophotometer (AA320N) and removal efficiency (%) for each metal was calculated as follows [14]:

$$RE\ (\%) = \frac{(C_o - C_f)}{C_o} \times 100 \qquad (1)$$

Where:

Co = concentration of adsorbate before interaction with adsorbent

C_f = concentration of adsorbate after interaction with adsorbent

Adsorption capacity of the AC at time t (q_t) was calculated using equation 2 (Musah *et al*., 2022):

$$q_t = \frac{(C_o - C_t)\, v}{m} \qquad (2)$$

Where:

v = volume of aqueous solution used for interaction

m = mass of adsorbent used

Adsorption Kinetics

The kinetics of adsorption was studied using the pseudo first order, pseudo second order, Natarajan-Khalaf first order, Bhattacharya-Venkobachar kinetics and intraparticle diffusion models [15]. The different kinetics models and equations are presented in Table 1

Table 1: Adsorption Kinetic Models and their Equations

Kinetic model	Equation
Pseudo first order	$\log (q_e - q_t) = \log (q_e) - \frac{K_t}{2.303} t$
Pseudo second order	$\frac{t}{q_t} = \frac{1}{k_2 q_e^2} + \frac{t}{q_e}$
Natarajan-Khalaf first order	$\log (\frac{Co}{Ct}) = (\frac{k}{2.303})t$
Bhattacharya-Venkobachar first order	$\log[U - U(T)] = -(\frac{k_B}{2.303})\, t$
Weber and Morris Intraparticle diffusion	$\log R = \log k_{id} + a \log (t)$
McKay and Poots Intraparticle diffusion	$q_t = k_1 t^{1/2} + X^1$

The equations take the form of equation of straight line i.e y = mx +c. For pseudo first order, the graph is a plot of log ($q_e - q_t$) against t while in the case of pseudo second order, it is 1/q_e versus t.

Results and Discussion

Results

Results of the effect of time on the adsorption of Cr^{6+}, Mn^{2+} and Pb^{2+} using *Vitellaria paradoxa* shell activated carbon (VPA) and *Mangifera indica* shell activated carbon (MIA) are presented in figure 1 (a and b) respectively while parameters for the adsorption kinetics and intraparticle diffusions are presented in Tables 2-7.

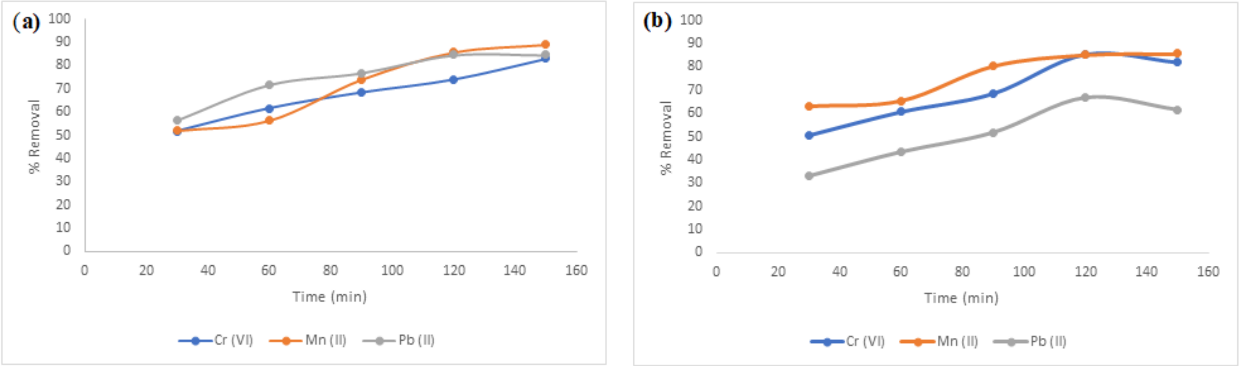

Figure 1: Percent removal of Cr^{6+}, Mn^{2+} and Pb^{2+} using (a) VPA and (b) MIA

VPA = *Vitellaria paradoxa* shell activated carbon MIA = *Mangifera indica* shell activated carbon

Table 2: Pseudo First Order Kinetic Parameters for the Adsorption of Cr^{6+}, Mn^{2+} and Pb^{2+}

Parameter	**Cr^{6+}**		**Mn^{2+}**		**Pb^{2+}**	
	VPA	**MIA**	**VPA**	**MIA**	**VPA**	**MIA**
R^2	0.9500	0.9770	0.9095	0.8591	0.3465	0.6353
k_1 (min^{-1})	0.0210	0.0212	0.0366	0.0152	0.0101	0.0108
qe,(exp)(mg/g)	0.0720	0.0710	0.3470	0.0350	0.0310	0.0220
qe,(cal) (mg/g)	0.0572	0.0572	0.7958	0.0162	0.0058	0.0098
SSE (%)	0.0067	0.0062	0.2007	0.0566	0.0114	0.0055

VPA = *Vitellaria paradoxa* shell activated carbon MIA = *Mangifera indica* shell activated carbon

Table 3: Pseudo Second Order Kinetic Parameters for the Adsorption of Cr^{6+}, Mn^{2+} and Pb^{2+}

Parameter	**Cr^{6+}**		**Mn^{2+}**		**Pb^{2+}**	
	VPA	**MIA**	**VPA**	**MIA**	**VPA**	**MIA**
R^2	0.9847	0.9698	0.9555	0.9758	0.9297	0.8557
k_2($mg.g^{-1}min^{-1}$)	0.3632	0.2892	0.0437	0.7973	0.4572	0.5248
qe,(exp)(mg/g)	0.0720	0.0710	0.3470	0.0350	0.0310	0.0220
qe,(cal) (mg/g)	0.0861	0.0925	0.4607	0.0426	0.0491	0.0334
SSE (%)	0.0063	0.0096	0.0509	0.0034	0.0081	0.0051

VPA = *Vitellaria paradoxa* shell activated carbon MIA = *Mangifera indica* shell activated carbon

Table 4: Natarajan and Khalaf First Order Kinetic Parameters for the Adsorption of Cr^{6+}, Mn^{2+} and Pb^{2+}

Parameter	Cr^{6+}		Mn^{2+}		Pb^{2+}	
	VPA	**MIA**	**VPA**	**MIA**	**VPA**	**MIA**
R^2	0.9713	0.8480	0.9592	0.9098	0.9354	0.8399
k (min^{-1})	0.0083	0.0101	0.0136	0.0092	0.0089	0.0055

Table 5: Bhattacharya and Venkobachar Kinetic Parameters for the Adsorption of Cr^{6+}, Mn^{2+} and Pb^{2+}

Parameter	Cr^{6+}		Mn^{2+}		Pb^{2+}	
	VPA	**MIA**	**VPA**	**MIA**	**VPA**	**MIA**
R^2	0.8558	0.7809	0.8648	0.9418	0.9431	0.7689
k_B (min^{-1})	0.0205	0.0282	0.0359	0.0355	0.0166	0.0198

Table 6: McKay - Poots Intraparticle Diffusion Parameters for the Adsorption of Cr^{6+}, Mn^{2+} and Pb^{2+}

Parameter	Cr^{6+}		Mn^{2+}		Pb^{2+}	
	VPA	**MIA**	**VPA**	**MIA**	**VPA**	**MIA**
R^2	0.9993	0.9232	0.9413	0.9255	0.9029	0.9029
k^1 ($mg/gmin^{1/2}$)	0.0037	0.0047	0.0239	0.0018	0.0016	0.0019
X_1 (mg/g)	0.0262	0.0188	0.0600	0.0139	0.0146	0.0028

Table 7: Weber - Morris Intraparticle Diffusion Parameters for the Adsorption of Cr^{6+}, Mn^{2+} and Pb^{2+}

Parameter	Cr^{6+}		Mn^{2+}		Pb^{2+}	
	VPA	**MIA**	**VPA**	**MIA**	**VPA**	**MIA**
R^2	0.9866	0.9417	0.9175	0.8925	0.9351	0.9439
k_{id}($mg.g^{-1}min^{-1}$)	0.0174	0.0143	0.0552	0.0103	0.0096	0.0030
N	0.5663	0.6627	0.7341	0.4942	0.5100	0.8514

Discussion of Results

Effect of effect of contact time on the adsorption of Cr^{6+}, Mn^{2+} and Pb^{2+}

The role of contact time in the study of adsorption arose from the necessity for identifying the rapidness at which adsorbates bind to adsorbent and removed from solutions and obtaining the optimal time for the highest adsorption of metal ions from wastewater. The relationship between contact time (30, 60, 90, 120 and 150 mins) of adsorbates with the adsorbents (VPA and MIA) and the percent adsorption of Cr^{6+}, Mn^{2+} and Pb^{2+} from mining wastewater is presented in Figure 1.

From Figure 1(b), it is obvious that the percentage removal of Cr^{6+}, Mn^{2+} and Pb^{2+} from the wastewater increased at the initial stages as contact time increases. Adsorption equilibrium was attained at 120 minutes when MIA adsorbent was used, after which there was no more increase in removal of Cr^{6+}, Mn^{2+} and Pb^{2+} with increase in contact time. At this point, the adsorbents have reached saturation state and further increase in time of contact between adsorbate and activated carbon will lead to the desorption of the adsorbates (Cr^{6+}, Mn^{2+} and Pb^{2+}) back into the solution. The rapid increase in the removal of metal ions at the initial stages of the process could be attributed to the vacant binding sites in the activated carbon [16].

Maximum of 81.30, 80.75 and 65.97 % of Cr^{6+}, Mn^{2+} and Pb^{2+} were adsorbed by MIA. The trend observed in adsorption is $Cr^{6+} > Mn^{2+} > Pb^{2+}$ when MIA used adsorbent. Similar trend was reported by Farghali et al. and Shaba et al. [16,17]. Differences in some properties of the activated carbon like pore size, pore volume and surface area could also contribute to adsorption pattern [18].

Adsorption Kinetics

The rate of adsorption of any molecule onto the surface of an adsorbent is an important factor in understanding the process of adsorption.

To demine the adsorption kinetics of Cr^{6+}, Mn^{2+} and Pb^{2+} onto *Vitellaria paradoxa* shell activated carbon (VPA) and *Mangifera indica* shell activated carbon (MIA), pseudo first order, pseudo second order, Natarajan and Khalaf first order, and Bhattacharya and Venkobachar first order models were employed. Intraparticle diffusion was also studied using McKay - Poots and Weber - Morris intraparticle diffusion model. A good correlation coefficient of kinetic data also helps in explaining the adsorption of ions onto adsorbent.

Pseudo first order model

The pseudo first order model is widely used model to describe the removal of adsorbate from liquid medium [14,19]. The amount of adsorbate removed from the medium, rate constant and correlation coefficients (R^2) for pseudo first order model of adsorption of Cr^{6+}, Mn^{2+} and Pb^{2+} are presented in Table 2. Slope and intercept of the plot of log $|q_e - q_t|$ versus time (*t*) was used to determine the pseudo first order rate constant and the theoretical quantity of adsorbate that was adsorbed per unit mass of AC

$|q_{e,\,cal}|$. Experimental q_e value $|q_{e,\,exp}|$ obtained for the adsorption of Cr^{6+}, Mn^{2+} and Pb^{2+} ranged between 0.0710 to 0.03470 mg/g with VPA having the highest adsorption capacity for Mn^{2+}. When the experimental q_e $|q_{e,\,exp}|$ is compared to the theoretical q_e $|q_{e,\,cal}|$, the result indicate that $q_{e\ exp}$ differs from $q_{e,cal}$ obtained from the linear plot of log $|q_e - q_t|$ versus t, indicative that the adsorption of Cr^{6+}, Mn^{2+} and Pb^{2+} onto VPA and MIA does not follow the pseudo first order model. These observations were similar to those reported by Mathew et al. and Shaba et al. [6,17] on the adsorption of heavy metals from pharmaceutical and electroplating wastewater.

Rate constants (k_1) obtained for the first order adsorption of Cr^{6+}, Mn^{2+} and Pb^{2+} onto VPA and MIA were low (0.0101 – 0.0366 min^{-1}) and the values for correlation coefficient (R^2) were also (0.3465 – 0.9770) lower than those obtained for pseudo second order (0.8557 – 0.9847) but values for the sum of square error (SSE) were high (seen in Table 2). High k_1 and R^2 with low SSE value depict a good fit of the model [18]. The low k_1 and R^2 values with high SSE obtained further corroborate pseudo first order model did not fit the experimental data, hence the adsorption of Cr^{6+}, Mn^{2+} and Pb^{2+} onto VPA and MIA did not follow pseudo first order kinetics.

Pseudo Second Order Model

The adsorption of Cr^{6+}, Mn^{2+} and Pb^{2+} onto VPA and MIA was verified using the pseudo second order model. The plots of *t/qt* against *t* presented were employed to determine the pseudo second order adsorption rate (k_2) and adsorption capacity (q_e) of the adsorbents. Values obtained were presented in Table 3. Values for pseudo second order rate constants obtained for removal of Cr^{6+}, Mn^{2+} and Pb^{2+} onto VPA and MIA adsorbents were between 0.0437 $mgg^{-1}min^{-1}$for adsorption of Mn^{2+} onto VPA to 0.7973 $mgg^{-1}min^{-1}$for adsorption of Mn^{2+} by MIA. These values were higher than those obtained for pseudo first order rate constant for removal of same metal ions onto same adsorbents. The higher the value of rate constant (k_2) the higher also is the removal of ions from solution [20]. This is supported by the high removal of Cr^{6+} onto VPA and MIA presented in figure 1. The k_2 values obtained were lower than the 0.7912 $mgg^{-1}min^{-1}$ obtained for removal of Ni^{2+}onto modified oil palm mesocarp fiber [17].

Correlation coefficients (R^2) for the pseudo second order kinetics on the adsorption of Cr^{6+}, Mn^{2+} and Pb^{2+} were between 0.8557 and 0.9847 for VPA and MIA respectively. These values were higher than those obtained for the pseudo first order model; the high pseudo second order correlation coefficient (R^2) values show that the adsorption process followed the pseudo second order model. Khamwichit et al. and Rout et al. [21,22], reported pseudo second order model as a good fit for describing adsorption process. Besides correlation coefficients (R^2), the applicability of pseudo second order model to the adsorption of Cr^{6+}, Mn^{2+} and Pb^{2+} onto VPA and MIA was tested using the sum of square error (SSE). The low SSE values (Table 3) confirm the adsorption process followed pseudo second order kinetic model.

Natarajan – Khalaf and Bhattacharya – Venkobachar First Order Kinetic Models

The linear form Natarajan - Khalaf first order kinetic is expressed using the equation [15,23]:
$log\ (C_o/C_t) = (K/2.303)t$

Where C_o and C_t being the concentrations (mg/dm^3) at times zero and t respectively. k was the Natarajan - Khalaf rate constant (min^{-1}) obtained from the slope of the plot of $log\ (C_o/C_t)$ against t. The values of the correlation coefficients (R^2) and rate constant (k) for the adsorption of Cr^{6+}, Mn^{2+} and Pb^{2+} are presented in Table 4. Rate constants (k) values obtained were between 0.0055 and 0.0101 min^{-1} and correlation coefficient (R^2) values were between 0.8399 and 0.9713. The values of rate constant of $log\ [1-U(T)]$ versus t (Venkobachar First Order) in the equation $log\ [1-U(T)] = -\ (K/2.303)t$ are presented in Table 5. The correlation coefficients (R^2) for adsorption of Cr^{6+}, Mn^{2+} and Pb^{2+} onto VPA and MIA were in the range of 0.7689 and 0.9418. These values were lower than those of pseudo second order but higher than values of pseudo first order model for the experiment. The low R^2 values of Natarajan and Khalaf first order, and Bhattacharya and Venkobachar first order models indicate the lack of fit of these models in describing the adsorption process and experimental data obtained, hence the adsorption process did not follow these orders. Similar R^2 values were obtained for the adsorption of Cd^{2+} and Cu^{2+} onto adsorbent prepared from agricultural wastes [23].

McKay and Poots Intraparticle Diffusion

This model is employed to determine adsorption mechanism. According to this model, the plot of uptake (q_t) versus the square root of time ($t_{1/2}$) would give a linear line if intraparticle diffusion is involved in the process for adsorption [24,25]. If the line goes through origin, then intraparticle diffusion is the rate limiting step. If the plot doesn't follow through the origin, then intraparticle diffusion on of the adsorbate is not the only rate controlling step but other kinetic models could be involved in the adsorption rate, and these parameters could all be operating concurrently [24,26].

The McKay and Poots equation is usually expressed as [27]:

$q_t = k_1t^{1/2} + X^1$ Where K_1 is the intraparticle diffusion rate constant (mg/gmin$^{1/2}$) and X^1 is the boundary layer diffusion effect.

Values of k_1 and X^1 were obtained from the slope of the plot of qt versus $t^{1/2}$ for the removal of Cr^{6+}, Mn^{2+} and Pb^{2+} onto VPA and MIA presented in Table 5. The initial curves in the plots are due to boundary layer diffusion effects and an extrapolation of the linear line to the time axis gives the intercept, X^1 is proportional to the thickness of the boundary layer [25,28]. Boundary layer provides the indication of the capacity of the activated carbons to adsorb ions from solutions and is also seen as a viscous drag that exist between the activated carbon surfaces and solution containing metal ions diffusing across the boundary layer [11,27].

X^1 values obtained for sorption Cr^{6+} onto VPA and MIA presented in Table 5 were 0.0262 and 0.0188 mg/g. Values of Pb^{2+} adsorption were 0.0146 and 0.0028 mg/g respectively. A high X^1 value correspond with great boundary thickness and indication of higher adsorption capacity [25]. From the results, the boundary layer thickness varies between 0.0600 and 0.0139 mg/g with the adsorption of Mn^{2+} onto VPA having the highest X^1 value (0.0600 mg/g) indicating high capacity of VPA for the adsorption of Mn^{2+}. The 0.0600 mg/g obtained for the adsorption of Mn^{2+} is higher than the 0.039 mg/g obtained for removal of Strontium from solution by activated carbon prepared from rice straw [26] but much lower than the 0.894 mg/g reported by Youssef *et al.,* [29] for the adsorption of lead. The thickness of a boundary layer decreases with increase temperature and this increases the tendency of the ions to desorb from the activated carbon (adsorbent) surface back to the solution phase resulting in a reduction in removal adsorbate from solution [11,25].

Weber and Morris Intraparticle Diffusion

The Weber - Morris model was employed to further study the intraparticle diffusion process of Cr^{6+}, Mn^{2+} and Pb^{2+} adsorption onto VPA and MIA. The linear expression of the model is [25,30].

$$\log q_t = \log k_{id} + n \log t$$

where k_{id} is the rate constant of intraparticle diffusion and n indicates the mechanism of adsorption. Values of k_{id} and n were gotten from plots as intercept and slope, and their values were presented in Table 7. The values obtained for the rate constant, k_{id} of intraparticle diffusion ranged from 0.0030 to 0.0552 $mgg^{-1}min^{-1}$ for the adsorption of Cr^{6+}, Mn^{2+} and Pb^{2+} onto VPA and MIA, while n values were between 0.492 and 0.7341 respectively. The rate constant, k_{id} (intercept) intraparticle diffusion gives an idea concerning the boundary layer thickness [31]. The larger the value of the intercept, the greater will be the effect of the boundary layer and an increase in the rate of adsorption [32,33]. The low values of k_{id} on Table 7 are indications of the presence of intraparticle diffusion as a rate determining step among other processes that control the rate of adsorption which may also be operating concurrently [27]. The 0.05525 $mgg^{-1}min^{-1}$ obtained for the adsorption of Mn^{2+} onto VPA is lower than the 0.0882 and 0.4450 $mgg^{-1}min^{-1}$ reported for the adsorption of titanium and cadmium respectively [34,35]. High n-values are indications of a better adsorption mechanism [27].

The n-values obtained (0.7341, 0.5663 and 0.5100) for adsorption of Mn^{2+}, Cr^{6+}, and Pb^{2} onto VPA are higher than the 0.0068, 0.0048 and 0.0125 reported for adsorption of Cd^{2+}, Pb^{2+} and Cu^{2+} onto modified cocoa pod husk [25]. The low correlation coefficients (R^2) of Weber and Morris intraparticle diffusion which are comparable to those obtained for McKay and Poots intraparticle diffusion model further confirmed that intraparticle diffusion of the adsorbate is not the only rate determining process.

Comparing the correlation coefficients (R^2) the models studied, results indicated low R^2 values for pseudo first order, Natarajan and Khalaf first order, Bhattacharya and Venkobarcha first order and intraparticle diffusion models but high correlation coefficients, R^2 values (> 0.9) for pseudo second model indicate that the pseudo second kinetic model gives a better fit to the experimental data than the other models. This is observation is similar to reports of [29,34] on the sorption of Cd (II) and U(VI) respectively.

Conclusion

Time of interaction between the adsorbent and the mining water had positive effect on the adsorption of Cr^{6+}, Mn^{2+} and Pb^{2+} onto VPA and MIA. Kinetic study of the experimental data for adsorption of Cr^{6+}, Mn^{2+} and Pb^{2+} onto VPA and MIA showed that pseudo second order model having correlation coefficient (R^2) greater than 0.99 is more suitable in describing the adsorption process than pseudo first order model, indicating the influence of film and pore diffusion mechanism during sorption. The very low sum of square error and the closeness of q_e (exp) to q_e (cal) further confirm the suitability of pseudo second order kinetic in describing the process.

References

1. Li, H., Xiao, D., He, H., Lin, R. & Zuo, P. (2012). Adsorption behaviour and adsorption mechanism of Cu (II) ions on amino-functionalized magnetic nanoparticles. *Transactions of Nanoferrous Metals Society of China*, 23,2657-2665.
2. Sumi, L. & Thomsen, S. (2001). Mining in remote areas: Issues and impacts. *Environmental Mining Council of British Columbia. MiningWatch Canada/Mines Alerte, Ottawa, Ontario.*
3. Sonone, S. S., Jadhav, S., Sankhla, S. L. & Kumar, R. (2021). Water Contamination by Heavy Metals and their Toxic Effect on Aquaculture and Human Health through Food Chain. *Letters in Applied NanoBioscience*, 10(2), 2148 – 2166.
4. Jhariya, D., Khan, R. & Thakur, G. S. (2016). Impact of mining activity on water resource: an overview study. *Proceedings of the Recent Practices and Innovations in Mining Industry, Raipur, India*, 19-20.
5. Babatunde, A. I., Bamgbola, E. P. & Oyalola, O. T. (2014). The pharmaceutical effluents on the quality of groundwater: a case study of Ikeja industrial area of Lagos, Nigeria. *International Journal of Medical Resources and Health Science*, 4(1),1-8.
6. Mathew, J. T., Musah, M., Azeh, M. & Mohammed, M. (2024). Development of Fe_3O_4 nanoparticles for the removal of

some toxic metals from pharmaceutical wastewater. *Caliphate Journal of Science & Technology*, 6(1), 26-34.

7. Musah, M., Mathew, J. T., Azeh, Y., Badeggi, U. M., Muhammad, A. I. and Muhammad, K. T. (2023). Intraparticle diffusion study of the adsorption of Ni^{2+} and Mn_{2+} onto chemically modified agricultural waste. Development Journal of Science and Technology Research, 13(1), 73-81.
8. Misihairabgwi, J. M., Kasiyamhuru, A., Anderson, P. Cunningham, C. J., Peshkur, J. A. & Ncube, I. (2014). Adsorption of heavy metals by agroforestry waste derived activated carbons applied to solution. *Africa Journal of Biotechnology*, 13(4),1579-1587.
9. Muhammad, M. S., Musah, M. and Mathew, J. T. (2024). Preparation and characterization of activated carbon from Africa star apple (*Chrysophyllum albidum*) seed shell. *FUDMA Journal of Sciences*, 8(3), 194-199.
10. Abdulkarim, M., Ibrahim, I. L., Mohammed, M. and **Musah, M.** (2024). Preparation and characterization of activated carbon from Date Palm *(Phoenix dactylifera)* seeds. *FUDMA Journal of Sciences*, 8(3), 409-415.
11. Ahmad, M. A., Puad, N. A. A. & Bello, O. S. (2014). Kinetic, equilibrium and thermodynamic studies of synthetic dye removal using pomegranate peel activated carbon prepared by microwave-induced KOH activation. *Water Resources and Industry*, 6,18-35.
12. Siti, K. C. O., Siki, F. C. O., Misnon, N. A. & Hanim, F.K. (2012). Utilization of sugarcane bagasse in the production of activated carbon for groundwater treatment. *Intrenational Journal of Engineering and Applied Science*, 1(2),76-85.
13. Ogunleye, I. O. & Izuagie, A. A. (2013). Determination of heavy metal content in some industrial effluents from Ondo State, Nigeria. *Journal of Envvironmental Chemistry and Ecotoxicology*, 5(8),216-219.
14. Mathew, J. T., Musah, M., Azeh, M. & Mohammed, M. (2023). Adsorptive Removal of Selected Toxic Metals from Pharmaceutical Wastewater using Fe_3O_4/ZnO Nanocomposite. *Dutse Journal of Pure and Applied Sciences*, 9(4a), 236-248.
15. Musah, M., Azeh, Y., Mathew, J. T., Umar, U. M., Abdulhamid, Z. & Muhammad, A. I. (2022). Adsorption kinetics and isotherm models: A Review. *Caliphate Journal of Science and Technology*, 4(1),20-26.
16. Farghali, A.A., Bahgat, M., Enaiet-Allah, A. & Khedr, M.H. (2013). Adsorption of Pb (II) ions from aqueous solutions using

Copper oxide nanostructures. *Journal of Basic and Applied Science*, 2,61-71.

17. Shaba, E. Y., Mathew, J. T., Musah, M., Mohammed, M., Muhammad, A. I. & Obetta, H. C. (2021). Adsorption of heavy metals from electroplating wastewater using guinea corn husk activated carbon. *Lapai Journal of Science and Technology*, 7(1),122-132.
18. Musah, M., Yisa, J., Suleiman, M. A. T., Mann, A., Shaba, E.Y. & Aliyu, A. (2018). Kinetics and isotherms studies of the adsorption of Cr^{6+}, Mn^{2+} and Cd^{2+} ions onto chemically modified *Bombax buonopozense* calyx. *Biological and Environmental Sciences Journal for the Tropics,* 15(1), 28-34.
19. Farouk, R. & Yousef, N .S. (2015). Equilibrium and kinetics studies of adsorption of Copper (II) ions on natural biosobent. *International Journal of Chemical Engineering and Application.* 6(5),310-324.
20. Edet, U. A. & Ifelebuegu, A. O. (2020). Kinetics, isotherms, and thermodynamic modelling of the adsorption of phosphates from model wastewater using recycled brick waste. *Processes,* 8,665,1-15.
21. Khamwichit, A., Dechapanya, W. & Dechapanya, W. (2022). Adsorption kinetics and isotherm of binary metal ion in aqueous solution using untreated Venus shell. *Heliyon*, 8,1-12.
22. Rout, S. kumar, A., Ravi, P. M. & Tripthi, R. m. (2015). Pseudo second order kinetic model for sorption of Uranium (VI) onto soil: A comparison of linear and non-linear methods. *International Journal of Environmetal Science*, 6(1),145-154.
23. Meera, M. S. & Ganesan, T.K. (2015). Adsorption isotherm and kinetics studies of cadmium (II) ions removal using various activated carbons derived from agricultural bark wastes: A comparative study. *Journal of Chemical and Pharmaceutical Research*, 7(4),1194-1200.
24. An, B. (2020). Cu (II) and As (V) Adsorption Kinetic Characteristic of the Multifunctional Amino Groups in Chitosan. *Process*, 1-15.
25. Odoemelam, S. A., Iroh, C. U. & Igwe, J. C. (2011). Copper (II), cadmium (II) and lead (II) adsorption kinetics from aqueous metal solutions using chemically modified and unmodified cocoa pod husk (*Theobroma cacao*) waste biomas. *Research Journal of Applied Sciences,* 6(1):44-52.
26. Yakout, S. M. & Elsherif, E. (2010). Batch kinetics, isotherm and thermodynamic studies of adsorption of strontium from aqueous solutions onto low-cost rise straw based carbons. *Carbon-Science and Technology*, 1,144-153.

27. Patil, S. D., Renukdas, S. and Patel, N. (2012). Comparative study of kinetics of adsorption of methylene blue from aqueous solutions using cinnamon plant (*Cinnamonum zeylanicum*) leaf powder and pineapple (*Ananas comosus*) peel powder. *The Electronic Journal of Chemistry*, 4(2),77-100

28.]Musah, M., Mathew, J. T., Azeh, Y., Badeggi, U. M., Abdulhamid, Z. & Muhammad, A. I. (2023). Kinetic studies of the adsorption of manganese (II) and nickel (II) ions onto modified oil palm mesocarp fiber. *Bima Journal of Science and Technology*, 7(1),47-53.

29. Youssef, A. M., Dawy, M. B., Akland, M. A. & Abou-Elanwar, A. M. (2013). EDTA versus nitric acid modified activated carbon for adsorption studies of lead (II) from aqueous solutions. *Journal of Applied Science Research*, 9(1),897-912.

30. Hasani, N., Selimi, T., Mele, A., Thaçi, V., Halili, J., Berisha, A. & Sadiku,M. (2022). Theoretical, equilibrium, kinetics and thermodynamic investigations of methylene blue adsorption onto lignite coal. *Molecules*, 1-19.

31. Ram-Prasath, R., Muthirulam, P. & Kannan, N. (2014). Agricultural wastes as low-cost adsorbents for the removal of acid blue 92 dye: A comparative study with commercial activated carbon. *IOSR Journal of Agriculture and Vetenary Science*, 7(2):19-32

32. Pholosi, A., Naidoo, E. B. & Ofomaja, A. E. (2020). Intraparticle diffusion of Cr (VI) through biomass and magnetite coated biomass: A comparative kinetic and diffusion study. *South African Journal of Chemical Engineering*, 32, 39-55.

33. Okewale, A. O, Babayemi, K. A., & Olalekan, A. P. (2013). Adsorption isotherms and kinetics models of starchy adsorbents on uptake of water from ethanol-water system. *International Journal Applied Science and Technology,* 3(1),35-42.

34. Javadian, H., Ghorbani, F. Tayebi, H. and Hosseini, S. M. (2015). Study of the adsorption of Cd (II) from aqueous solution using zeolite-based geopolymer synthesized from coal fly ash; kinetic, isotherm and thermodynamic studies. *Arabian Journal of Chemistry*, 8:837-849.

35. Ekwumengbo, P. A., Kagbu, J. A., Nok, A. J. & Omoniyi, K. I. (2010). Kinetics of gamma globulin adsorption onto titanium. *Rasaya Journal of Chemistry*, 3(2),221-231.